P1.1

SIMULATION TESTBED FOR ATMOSPHERIC LIDAR APPLICATIONS

Hilary E. Snell*, J. Stewart Hager, T. Scott Zaccheo
Atmospheric and Environmental Research, Inc., Lexington, Massachusetts

AER is developing a testbed capable of simulating lidar sensors, such as those used for Differential Absorption LIDAR ("DIAL") measurements. The testbed is designed for maximum flexibility to allow for the rapid prototype and development of trace gas remote sensing systems. The input atmospheric profile set (used to specify the temperature, moisture and molecular constituent profiles) is constructed from actual numerical weather prediction (NWP) model fields drawn from a global database of model outputs. The testbed has the capability of perturbing these input model fields to simulate errors in the specification of the atmospheric state or to provide a set of test cases spanning a wide range of conditions with realistic, but highly variable, structure. The profiles are used in conjunction with automated LBLRTM runs for line-by-line optical depth calculations over the desired spectral region. LBLRTM can also be coupled with the CHARTS multiple scattering code for cases requiring multiple scattering calculations (aerosols and clouds). The input parameters include sensor altitude, viewing geometry, surface altitude and reflectivity, and cloud/aerosol parameters (such as density, location and specific phase functions). Additional inputs included in the testbed are sensor-related parameters such as the laser line shape, detector noise and laser wavelength stability. The testbed may be coupled to various geophysical parameter retrieval algorithms, including those specific to the DIAL technique. The geophysical parameter retrievals can then be computed and compared with the truth. This paper will describe the testbed architecture and the process by which the input NWP profiles are generated, and will provide example LIDAR simulations for trace gas retrievals with a DIAL system.

1. INTRODUCTION

The technique of light detection and ranging ("lidar") is a powerful tool for environmental monitoring. Lidar allows measurements of the concentration of atmospheric constituents to be made over large areas in real time, with good spatial resolution. The technique is based on interaction of laser light with atmospheric constituents. A priori unknown or approximately known quantities such as instrument constants, receiver efficiency, target reflectivity and atmospheric backscattering affect this interaction of laser light with the atmosphere. To cancel these factors one can use a differential absorption lidar ("DIAL") technique whereby two wavelengths are used to characterize the constituent of interest and the background. In practice two different wavelengths are selected such that while the first one is the resonance with the peak ("on") an absorption line of the species under investigation, the second is tuned away from ("off") the peak. In this configuration the backscattered signals have different intensities due only to the constituent of interest, and the ratio of the corresponding signals leads directly to an estimate of the concentration of the species under study. The two frequencies must be carefully selected to prevent interference from other atmospheric molecule absorption lines, minimize temperature dependence and optimize optical depth.

We have developed a computer testbed for use in the simulation of potential DIAL sensor configurations. The core of the testbed is the atmospheric radiative transfer module supplied by the LBLRTM (Line-By-Line Radiative Transfer Model) (Clough et al., 2005), which is highly accurate and well validated. Further, the line-by-line (monochromatic) calculation is suitable for laser applications. We will use the middle infrared region to demonstrate this testbed, but LBLRTM, and this testbed, is applicable from the microwave through the ultraviolet region of the spectrum.

2. TESTBED STRUCTURE

Our testbed has been designed to allow for the simulation of realistic atmospheric conditions. To this end the models require temperature, water vapor and trace gas concentrations as a function of atmospheric pressure through the line-of-sight.

**Corresponding author address*: Hilary E. Snell, Atmospheric and Environmental Research, Inc., Lexington, MA 02421-3126; e-mail: hsnell@aer.com.

As discussed below we have developed a method to generate arbitrary, realistic profile information using numerical weather prediction (NWP) models. These profile sets contain realistic, representative error statistics based on differences in NWP forecasts.

The testbed is designed to be flexible in terms of both the spectral region of interest and the types of profiles for which the simulation is conducted. The user also has control over the range of sensor altitudes (for ground-, aircraft- and space-based simulations).

The input profiles consist of a custom profile set generated from either NWP data, TIGR3 profiles or ECMWF profiles. The NWP-based profiles are created using the method described by Zaccheo and Snell (2006). In this procedure six hour forecast calculations are checked against actual conditions six hours later in order to compute a covariance matrix. The profile set is determined by specifying the mean profile and allowing the covariance matrix to constrain the variability of the set of perturbed ("test") profiles. This gives a simulation of the profile variability that is true to nature with the specified variance. For a typical set of lidar simulations, three hundred profiles are simulated using this technique, as shown in Figure 1. Note that 300 profiles were chosen as a trade-off between overall variability and required calculation time. In practice this number could be increased for more extensive testing.

Two additional profile sets can be used within the testbed for testing lidar simulations: the TIGR-3 (Thermodynamic Initial Guess Retrieval, version 3) dataset (shown in Figure 2), and the ECMWF (European Centre for Medium-Range Weather Forecasting) profiles (shown in Figure 3). This allows for direct comparison to other sensor simulations done on those profile sets. The profiles are typically characterized by latitude: above 50 degrees is considered high latitude, between 50 degrees and 30 degrees is considered mid-latitude, and below 30 degrees is considered tropical. The profile sets can be used as-is or perturbed using the NWP-derived covariance. Three profiles are chosen from the databases and perturbed in the same way as the NWP profiles.

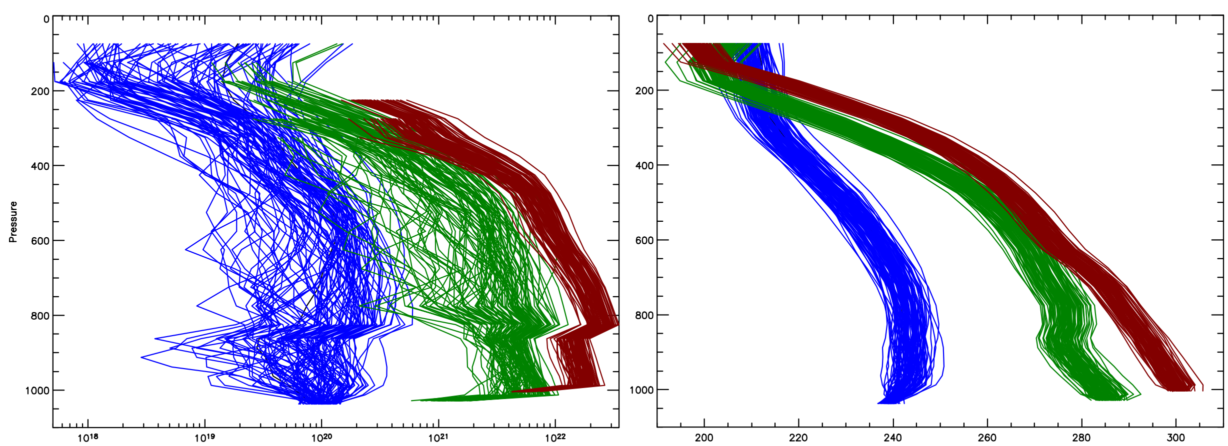

Figure 1: NWP testbed profiles: From left to right the profiles are representative of high-latitude, mid-latitude and tropical atmospheres.

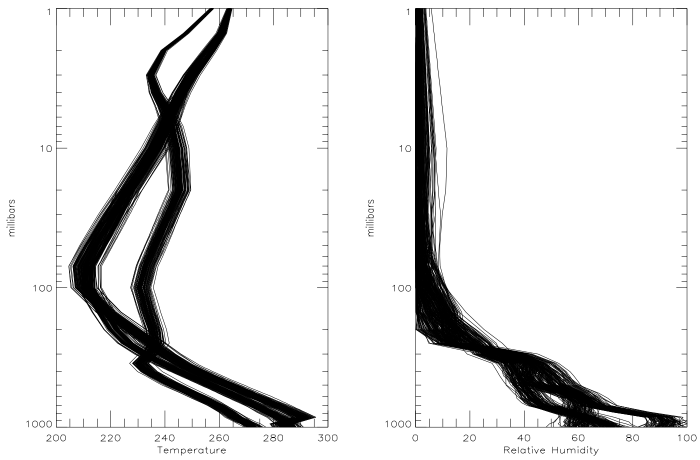

Figure 2: TIGR testbed profiles: From left to right the profiles are representative of high-latitude, mid-latitude and tropical atmospheres.

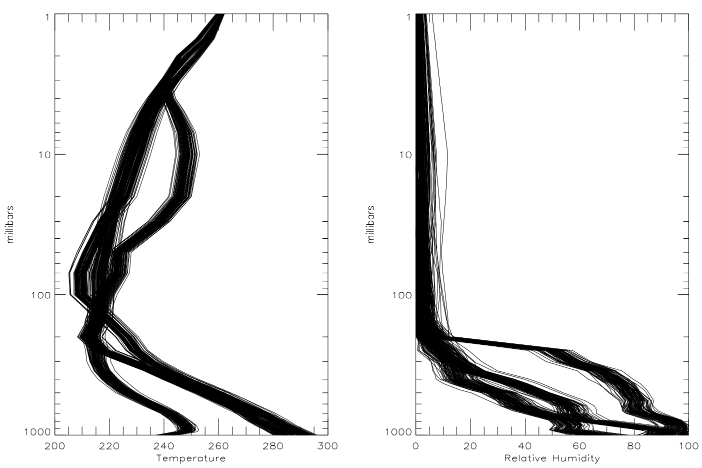

Figure 3: ECMWF testbed profiles: From left to right the profiles are representative of high-latitude, mid-latitude and tropical atmospheres.

The testbed is constructed to use the assembled profile data compute the layer quantities used as input to LBLRTM for calculation of monochromatic optical depths. The layer optical depths are then combined to compute the path transmittances. This provides flexibility for changing geometry parameters and sensor wavelengths without having to re-compute the optical depths.

The differential lidar technique uses measurements at specific spectral locations to retrieve column abundances. The specific spectral wavelengths are selected so that the gas being measured has a higher absorption coefficient at the “on” line position than the “off” line position. Lidar signals at the 'on' and 'off' line frequencies are characterized by the equations:

$$P_{off}\left(z\right)=\frac{C_{off}\eta_{off}\left(z\right)\beta_{off}\left(z\right)T_{off}\left(z\right)}{z^2} * \exp\left[-2\sigma_{off}\int_0^z\rho\left(z'\right)dz'\right] \quad (0.1)$$

$$P_{on}\left(z\right)=\frac{C_{on}\eta_{on}\left(z\right)\beta_{on}\left(z\right)T_{on}\left(z\right)}{z^2} * \exp\left[-2\sigma_{on}\int_0^z\rho\left(z'\right)dz'\right] \quad (0.2)$$

where *P(z)* is the Lidar signal backscattered from range *z*, *C* is the instrument constant, η is the receiving efficiency of the Lidar, β is the atmospheric backscattering coefficient, *T* is the two-way atmospheric transmission excluding gas species of interest, σ is the absorption coefficient of the species of interest, and ρ is the species of interest concentration. Taking the ratio of $P_{off}(z)$ to $P_{on}(z)$ and subsequently the logarithm of the ratio, we obtain:

$$\ln\left(\frac{P_{off}}{P_{on}}\right) = \ln\left(\frac{C_{off}}{C_{on}}\right) + \ln\left(\frac{\eta_{off}}{\eta_{on}}\right) + \ln\left(\frac{\beta_{off}}{\beta_{on}}\right) + \ln\left(\frac{T_{off}}{T_{on}}\right) + 2\left(\sigma_{on} - \sigma_{off}\right)\int_0^z \rho\left(z'\right)dz' \quad (0.3)$$

Because the 'off' and 'on' frequencies are relatively close, the first four terms on the right side of the equation can be neglected (Zhao, 2000).

Solving (0.3) for column abundances:

$$\int_0^z \rho\left(z'\right)dz' = \frac{1}{2\left(\sigma_{on} - \sigma_{off}\right)}\ln\left(\frac{P_{off}}{P_{on}}\right) = N \quad (0.4)$$

where N is total number of molecules per cm^2. Solving equation (0.4) requires values for the absorption coefficients (σ) and the return signals (P). The absorption coefficients are determined by solving Beer's law equation

$$T\left(\nu\right) = \exp\left[-\sigma\left(\nu\right)\cdot 2N\right] \quad (0.5)$$

for the absorption coefficient for an assumed atmospheric profile, where $T(\nu)$ is the transmission of the gas of interest:

$$\sigma\left(\nu\right) = \frac{-1}{2N}\ln\left[T\left(\nu\right)\right] \quad (0.6)$$

Because the absorption coefficients are calculated using the transmissions and column abundances of the simulated atmosphere they are *virtual absorption coefficients*, indicating they are not the actual absorption coefficient specific to the measurement, but a value that is used to retrieve column amounts in the DIAL equation. For actual measurements one must carefully select the virtual absorption coefficient so that it is representative of the atmospheric state (to avoid introducing errors into the retrieval). For simulation purposes it is sufficient to use a virtual absorption coefficient representative of the mean of the simulation profiles. Once the absorption coefficients have been chosen, they are placed in to the DIAL equation and used to calculate the column abundances.

3. APPLICATION

The AER lidar testbed has been applied to a variety of trace gas remote sensing problems. As an example, consider the measurement of CO2 abundance.

For observations of CO_2 mixing ratios a measurement precision equivalent to three part per million by volume or better is desired to determine spatial gradients of CO_2 from which sources and sinks can be derived and quantified and then separated from seasonal fluctuation component. The current study was undertaken to evaluate the potential of a LIDAR system to measure changes as small as three ppm from a high altitude or space platform.

The objective of the line selection for DIAL applications is to find ranges that would minimize retrieval errors while maximizing absorption sensitivity. Thus we must first identify CO_2 infrared transitions with appropriate strengths for both tropospheric sounding and for the entire atmosphere that are relatively free of interference from other atmospheric constituents and least susceptible to temperature variations. One of these regions is the 1.6 μm (6000 – 6500 cm^{-1}) region.

Four major bands of CO_2 in the 6000 – 6500 cm^{-1} region of the infrared spectrum were chosen for analysis of retrieval errors. All four are the $3\nu_1 + \nu_3$ combination band of CO_2 with different Fermi resonances. The two strongest bands have absorption lines ranging from 6200 – 6250 cm^{-1} and 6320 – 6370 cm^{-1}. Also there are weaker bands from 6040 – 6110 cm^{-1} and 6460 – 6540 cm^{-1} on the lower and higher wavenumber sides of the two strongest bands.

Because we are able to examine the retrieval performance using a set of realistic atmospheric profile, we are able to evaluate the retrieval performance under a variety of atmospheric conditions. This allows for the analysis of line selection versus sensitivity to temperature and water vapor profile variability. As an example, Figure 4 shows the transmission and standard deviation for two CO2 lines. The standard deviation represents the change in transmission due only to changes in the water vapor and temperature profiles. The overall standard deviation of R(16) is greater than R(26), but the standard deviation has a trough at the center line of R(16), whereas R(26) has a peak. The standard deviation of the R(16) line is mainly due to broadening effects and therefore does not effect the center line; the standard deviation of the R(26) line comes at the line center. The broadening effects that produce the largest standard deviation come from the steepest part of the absorption line. The two vertical lines in each plot represents a

1GHz width. If one has a 1GHz or less laser line width then one could greatly reduce the standard deviation of R(16) "on" frequency. In this study the use of these lower J value lines has produce retrievals well below the three ppm threshold.

Temperature and pressure sensitivity analysis of DIAL measurement have been explored by several recent publications (Browell et al., 1991; Ambrico et al., 2000; Menzies and Tratt, 2003). In these publications the main focus is the temperature and pressure sensitivity of the DIAL "on" frequency and the DIAL "off" temperature and water vapor sensitivity is neglected. Our results (Figure 5) indicate that the best retrievals have "on" and "off" frequencies with the same order of standard deviation. Consequently the standard deviation of the "off" frequency cannot be neglected.

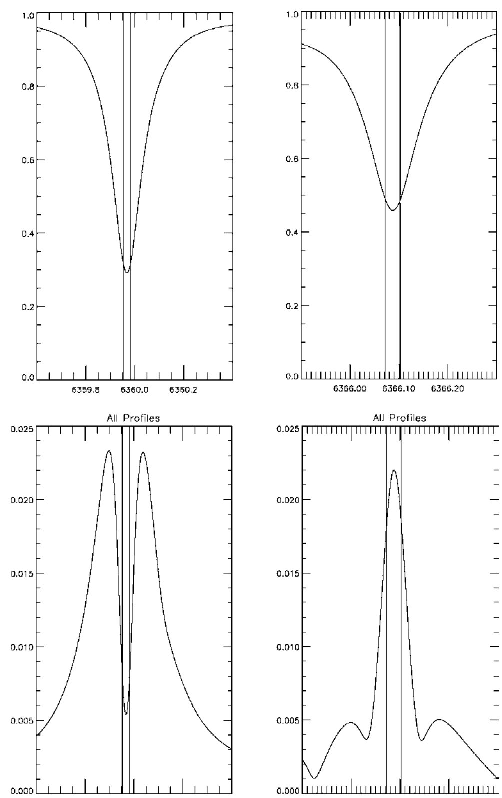

Figure 4: The transmission (upper panel) and standard deviation (lower panel) for two CO2 lines computed over a range of atmospheric profiles.

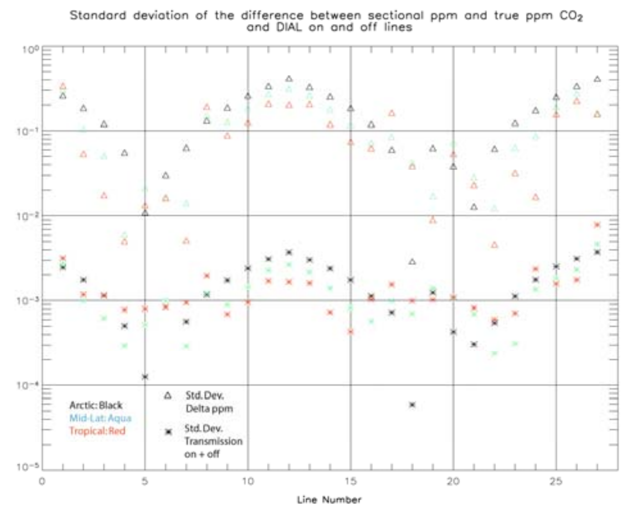

Figure 5: figure showing retrieval performance

4. CONCLUSION

The AER lidar simulation testbed is a robust tool that allows for a variety of lidar retrieval studies. The code as been constructed in a modular fashion to allow for maximum flexibility with regard to selection of test profiles, sensor geometric configuration and retrieval methodology. The use of LBLRTM to generate monochromatic optical depth files provides a consistent set of physics throughout the spectrum, from the microwave through the ultraviolet. In addition to understanding the sensitivity of specific laser wavelengths to variation in the temperature and water vapor profile, the testbed may also be used to understand sensitivity to other factors, such as surface pressure and cloud top pressure.

5. REFERENCES

Ambrico, P.F., A. Amodeo, P. Di Girolamo, and N. Spinelli, "Sensitivity analysis of differential absorption lidar measurements in the mid-infrared region," Appl. Opt. 39, 6847--6865 (2000).

Browell, E.V., S. Ismail, and B. E. Grossmann, "Temperature sensitivity of differential absorption lidar measurements of water vapor in the 720-nm region," Appl. Opt. 30, 1517--1524 (1991).

Clough, S. A., M. W. Shephard, E. J. Mlawer, J. S. Delamere, M. J. Iacono, K. Cady-Pereira, S. Boukabara, and P. D. Brown, 2005: Atmospheric Radiative Transfer Modeling: a Summary of the AER Codes. *J. Quant. Spectrosc. Radiat. Transfer*, **91**, 233-244.

Menzies, R.T., and D.M. Tratt, "Differential laser absorption spectrometry for global profiling of tropospheric carbon dioxide: selection of optimum sounding frequencies for high-precision measurements," Appl. Opt. 42, 6569--6577 (2003).

Zaccheo, T.S. and H.E. Snell, Requirements for Satellite-based Pressure Retrievals: Comparison of Global Surface Pressure Forecasts with In-Situ Measurements, in preparation, 2006.

Zhao, Y., "Line-pair selections for remote sensing of atmospheric ammonia by use of a coherent CO_2 differential absorption Lidar system," *Applied Optics* **39**, 997-1007 (2000).

6. ACKNOWLEDGEMENTS

This work was supported in part by a grant from ITT A/CD as well as AER internal research and development funds. The authors would like to thank Mike Dobbs (ITT), Berrien Moore (UNH) and Ron Isaacs (AER).